Experimental Determination of Rate of Energy Loss for Slow H^1, H^2, He^4, Li^6 Nuclei in Au and Al*

HOWARD A. WILCOX**
Institute for Nuclear Studies and Department of Physics, University of Chicago, Chicago, Illinois
(Received August 5, 1948)

A description is given of the use of a variable energy source of monoenergetic H^1, H^2, He^4, Li^6 nuclei, an energy analyzer, and an electron multiplier tube to measure the decrease in energy of these particles as they pass through a Au foil of known thickness; the measurements are carried out for protons from an energy of 30 kev to 400 kev, for deuterons from 30 kev to 650 kev, for alpha-particles from 30 kev to 1400 kev, and for the Li^6 nuclei from 750 kev to 850 kev. Similar measurements are carried out for the energy loss of protons and deuterons in Al over the energy range from 60 kev to 300 kev. Integrated range energy curves are given for these low energies. Although current theory predicts that the energy loss rates will be precisely equal for protons and deuterons of the same velocity, it is found that the loss rate for deuterons of low velocity is a few percent higher than that for protons of the same velocity. A qualitative explanation for the discrepancy is advanced.

I. INTRODUCTION

IT is of particular interest to determine the rate of energy loss by low velocity charged particles traversing material media, because present knowledge concerning this problem is both theoretically crude and experimentally meagre. A survey of the relevant literature shows that when the particle moves at such high velocity that it carries with it no bound electrons, the corresponding theory is accurate and well known,[1] but that when the particle moves slowly enough to carry with it some electrons in its various bound orbits, the theory becomes more qualitative.[2] Similarly, although much experimental work has been done on the velocity-energy loss relations for high energy protons and alpha-particles in various media,[3] very little has been attempted in the low energy regions,[4] probably because of the experimental difficulties encountered in detecting slow particles with the conventional Geiger counters, ionization chambers, and photographic plates.

The electron multiplier tubes, recently developed at this laboratory by J. S. Allen and used here to investigate the energy spectra of the recoil nuclei from the reactions $Be^9(p,d)Be^8$, $Be^9(p,\alpha)Li^6$, $H^2(d,n)He^3$, and $H^2(d,p)H^3$,[5-7] form an ideal tool for detecting very low energy particles, and have made possible these investigations of the velocity-energy loss relations for low energy particles in various media. This paper describes the experimental methods used in these investigations, together with the results now available.

II. THE EXPERIMENTAL METHODS

Figure 1 is a schematic diagram of the experimental arrangement. All the apparatus to the left of the "exit slit from target chamber" is used for the purpose of producing nearly monoenergetic, variable energy beams of the various kinds of particles under study, directed out to the right through this slit. On the other hand, all the

* The construction of the electron multiplier tube for this work was assisted by the joint program of the Office of Naval Research and the Atomic Energy Commission.
** Present address: Department of Physics, University of California, Berkeley, California.
[1] For a derivation of the basic formula, see N. Bohr, Phil. Mag. **25**, 10 (1913); H. A. Bethe, Ann. d. Physik **5**, 325 (1930); F. Bloch, Ann. d. Physik **16**, 285 (1933). For a correction at relativistic velocities, see H. A. Bethe, Zeits. f. Physik **76**, 293 (1932); C. Møller, Ann. d. Physik **14**, 531 (1932). For corrections due to K and L electron binding in the medium, see H. A. Bethe, Rev. Mod. Phys. **9**, 264 (1937); J. O. Hirschfelder and J. L. Magee, Phys. Rev. **73**, 207 (1948). For corrections in condensed media, see E. Fermi, Phys. Rev. **57**, 485 (1940); O. Halpern and H. Hall, Phys. Rev. **73**, 477 (1948).
[2] N. Bohr, Phys. Rev. **59**, 270 (1941); W. E. Lamb, Phys. Rev. **58**, 696 (1940); J. Knipp and E. Teller, Phys. Rev. **59**, 659 (1941).
[3] H. A. Bethe, Rev. Mod. Phys. **9**, 261 (1937).
[4] P. M. S. Blackett and D. S. Lees, Proc. Roy. Soc. **134**, 658 (1932); D. B. Parkinson, R. G. Herb, J. C. Bellamy, and C. M. Hudson, Phys. Rev. **52**, 75 (1937); C. M. Crenshaw, Phys. Rev. **62**, 54 (1942).
[5] For the Be reactions, see L. Del Rosario, Phys. Rev. **74**, 304 (1948).
[6] For the $H^2(d,n)He^3$ reaction, see H. V. Argo, Phys. Rev. **74**, 1293 (1948).
[7] The $H^2(d,p)H^3$ reaction is not yet published.

apparatus to the right of the "foil" in Fig. 1 is used for the purpose of measuring the distribution in energy of the beams of particles entering the analyzer mouth.

The idea of these experiments is the following: the apparatus is made to produce a nearly monoenergetic beam of the desired kind of particles, at some desired energy E_1, directed from the exit slit of the target chamber toward the mouth of the energy analyzer. With the foil swung out of this beam, the energy spectrum of the particles is investigated with the energy analyzer and is found to give a sharp maximum at the energy E_1. With the foil swung into the beam, the energy spectrum of the emergent particles is again investigated; the maximum is found at a lower energy E_2, and, since the thickness of the foil is not exactly constant, the energy spectrum of the emergent particles is somewhat broadened. The average energy lost in the foil by the particles is therefore $\Delta E = E_1 - E_2$. The average thickness Δx of the foil is measured, and the ratio $\Delta E/\Delta x$ gives the average rate at which the particles lose energy in the foil material. The average energy of the particles in the foil is taken to be $E = \frac{1}{2}(E_1 + E_2)$, and $\Delta E/\Delta x$ is measured as a function of E.

A. The Kevatron

The kevatron is the 400-kv Cockcroft-Walton accelerator, recently rebuilt in this laboratory and described elsewhere.[5] The accelerating voltage produced by this machine is measured using a high voltage resistance column whose value is known to ± 0.2 percent. Although the accelerating voltage tends to fluctuate slightly, it can be held always within ± 500 volts of any desired average value by means of continuous hand adjustment of a Variac feeding the primary of the high voltage transformer in the kevatron circuit.

The machine may be made to give useful beams of H^+, H_2^+, D^+, D_2^+, and He^+ ions with energies variable from about 40 kev to about 430 kev under average conditions. The desired beam is magnetically selected from the others, deflected through about 15°, and directed toward the target chamber. The beam charge which enters the target chamber is collected on the target and recorded by a beam current integrator of conventional design.

B. The Source of Particles

Two methods, the "scattering method" and the "reaction method," have been used to produce beams of the desired kinds of particles, at the desired energies, directed out through the exit slit from the target chamber.

1. The Scattering Method

In this method, the kevatron beam is limited at the entrance to the target chamber by a

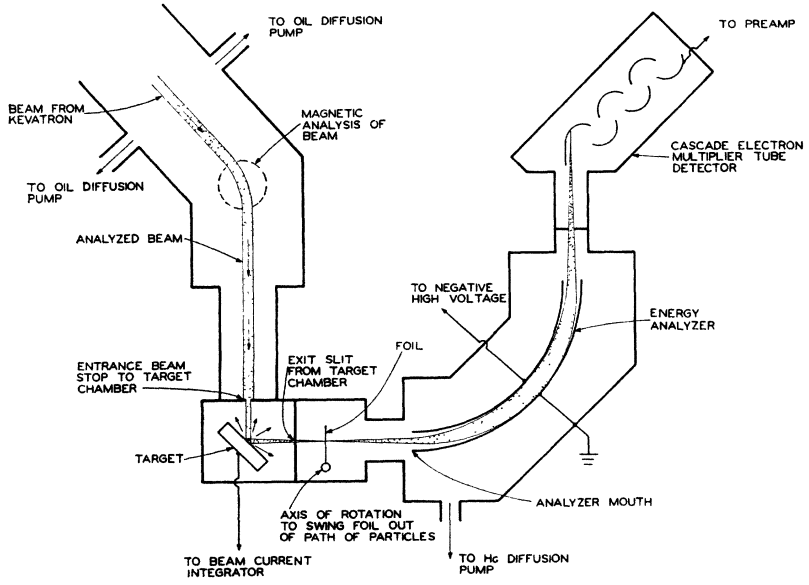

FIG. 1. Schematic diagram of experimental arrangement.

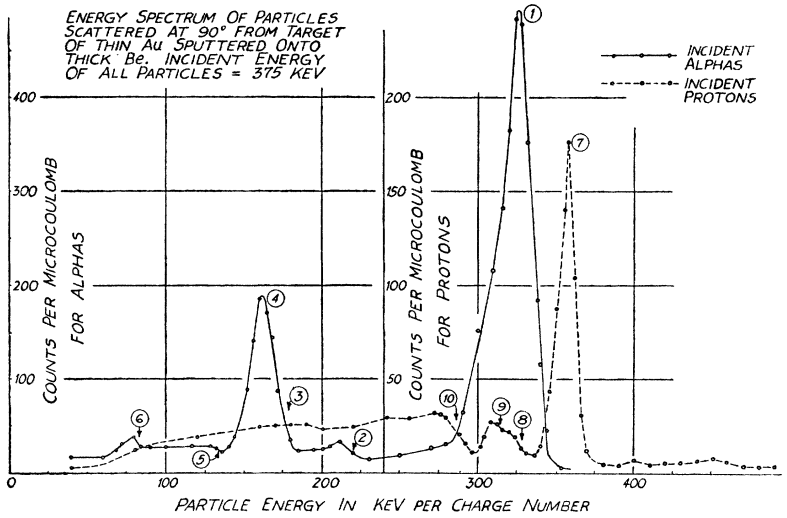

FIG. 2. Energy spectra of particles scattered at 90° from "scattering target" (see text). Peak 1 is He^+ coming from the thin Au layer, 2 is probably He^+ from an O layer, 3 is He^+ from a C layer, 4 is He^{++} from the Au layer, 5 is He^+ from the Be base, 6 is He^{++} from the C layer; peak 7 is H^+ from the Au layer, 8 is probably H^+ from an O layer, 9 is H^+ from a C layer, 10 is H^+ from the Be base. For explanation of presence of C on target see reference 9.

2.08-mm diameter drill hole in the beam stop. After passing through this hole, the ions impinge on the target, which is a solid Be disk with a very thin sputtering of Au on the polished front surface. The kevatron beam is incident on this target at 45°, and those particles which scatter at 90° from the incident beam into the direction of the exit slit are the useful particles.

If the particles in the beam have mass number A and energy E_B, then those which leave the exit slit after scattering from the very thin Au surface layer will *all* have energy

$$[(197-A)/(197+A)]E_B \quad \text{(mass number of Au}=197), \quad (1)$$

whereas those which leave the exit slit after scattering from the thick Be base will all have energies *less* than

$$[(9-A)/(9+A)]E_B \quad \text{(mass number of Be}=9). \quad (2)$$

Thus the energy spectrum of the particles leaving the exit slit from the target chamber exhibits a sharp maximum at the energy given by (1), as is desired for these experiments.[8] Figure 2 gives typical energy spectra curves of particles scattered from this target. (When these curves were taken, the target had a slight but visible deposit of carbon on it where the beam struck;[9] evidence for the presence of this carbon layer on the surface of the target is also to be seen in the energy spectra of Fig. 2.)

2. *The Reaction Method*

In this method, a beam stop with a 3.18 mm $\times$12.7 mm slit is used at the entrance to the target chamber, and the scattering target is replaced by a target which is a solid disk of Ni with a very thin layer of Be evaporated onto its polished front surface. This target is bombarded with protons, which produce the nuclear reactions $Be^9(p,d)Be^8$ and $Be^9(p,\alpha)Li^6$. Because of the high probability of these reactions, together with the extreme thinness of the Be layer on the Ni disk, the target becomes a fairly strong source of monoenergetic H^2, He^4, and Li^6 nuclei having kinetic energies of about 645 kev, 1400 kev, and 900 kev, respectively. In order to vary these energies somewhat, a second foil is inserted between the target and the exit slit from the target chamber. This foil is so arranged that it

[8] I am indebted to Dr. S. K. Allison for the suggestion of this kind of target.

[9] Since the accelerator tube is evacuated by two large oil diffusion pumps working in parallel, some oil vapor finds its way into the target chamber and tends to deposit on the surface of the target. When the beam strikes this deposit, the oil molecules are dissociated and inert carbon begins to build up. To help prevent oil vapor from reaching the target chamber, each pump is equipped with a liquid air trap and the walls of the long (30") beam entrance canal, terminating in the beam stop at the entrance to the target chamber, are cooled with solid CO_2. Furthermore, to help prevent any oil vapor in the target chamber from settling on the target, the latter is heated to a temperature just below that at which the adjacent brass begins to emit zinc vapor. These expedients are fairly successful, but nevertheless some carbonization of the targets is observed after prolonged bombardment.

may be rotated and its effective thickness thereby changed, thus varying the energies of the particles leaving the exit slit. Since this foil is used merely to control the energies of the particles produced in the "reaction method," its material and thickness are of no consequence and need not be known with any precision.

C. Foils

In the experiments so far completed, two foils of Au and one foil of Al were used. The Au foils were both cut from the same large sheet of Au, whose weight was $W=18.7\pm0.1$ mg and whose area was $A=99.99\pm1.21$ cm^2. Hence the average

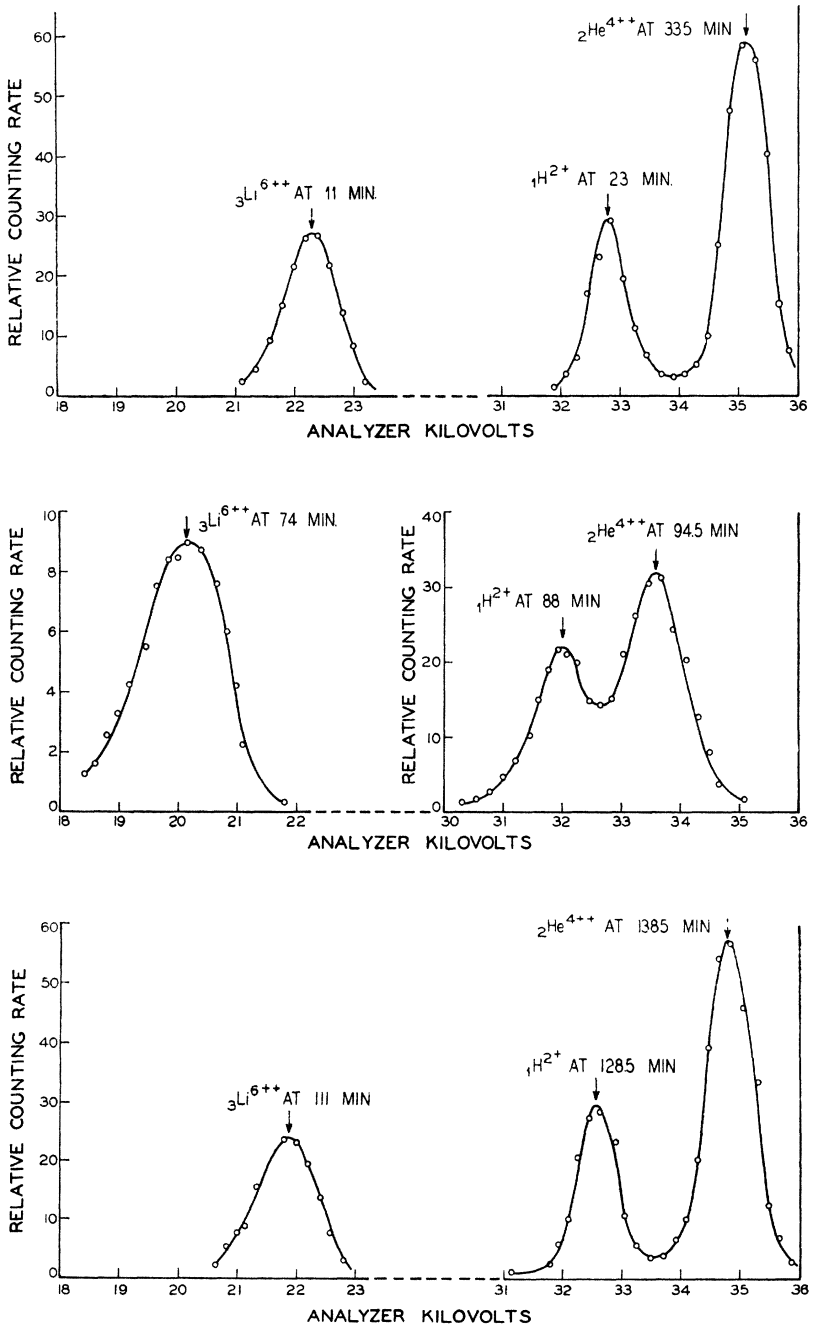

FIG. 3. Typical data from the "reaction method" (see text). Top curve is spectrum of particles without foil, middle curve is spectrum of particles emerging from Au foil, bottom curve is spectrum without foil again. Difference between top and bottom curves is due to progressive carbonization of target as explained in reference 9.

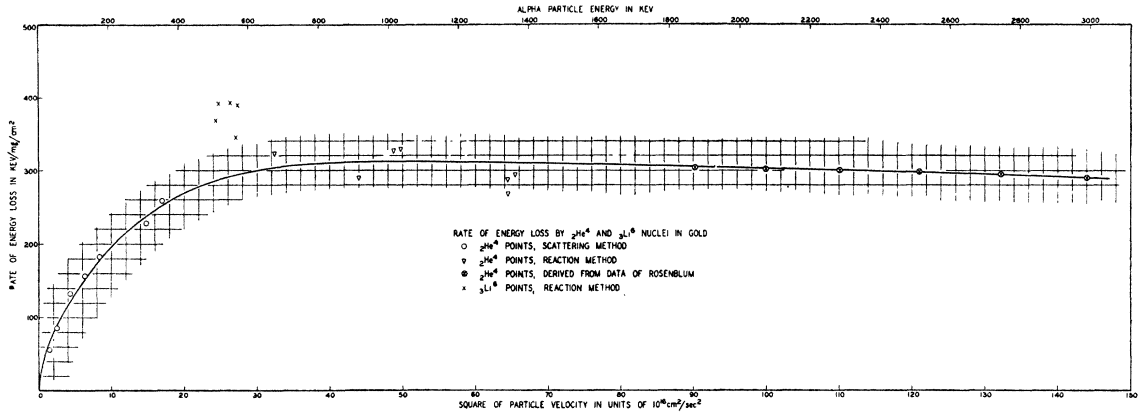

FIG. 4. Energy loss rates for He^4 and Li^6 nuclei in Au. The Li^6 energies range from 750 kev to 880 kev.

surface density of this sheet was

$$W/A=(18.7\pm0.53\%)/(99.99\pm1.21\%)$$
$$=0.187\pm1.74\%\ \text{mg/cm}^2.$$

This figure is probably reliable for both foils within the limits of error indicated, since beaten Au foil is very uniform. On the other hand, it was found that the available Al foil was not of uniform thickness. A 9.54-mm×19.1-mm portion of Al foil was used in these experiments, and subsequently a 6.35-mm disk was cut from the center of this portion, its diameter was measured with a micrometer microscope, and its weight was measured with a microbalance. The weight of this disk was $W=0.0543\pm2.8$ percent mg and the area of the disk was $A=0.317\pm1.0$ percent cm^2; hence the surface density of the Al foil used in these experiments was

$$W/A=(0.0543\pm2.8\%)/(0.317\pm1.0\%)$$
$$=0.171\pm3.8\%\ \text{mg/cm}^2.$$

To minimize the danger that vapor from the pumps will condense on the foils, the apparatus is set up so that the foil chamber and energy analyzer can be sealed off by stopcocks at the exit slit from the target chamber and at the pump outlet from the energy analyzer. By means of these arrangements, the foils are left in the static vacuum of the energy analyzer except during the actual running times of the experiments.

D. The Energy Analyzer

The energy analyzer used in these experiments is the same one used by L. Del Rosario and others; its description appears in the literature,[10] and will be only briefly summarized here. The analyzer (see Fig. 1) is a pair of quarter-circle, cyclindrical, concentric aluminum surfaces, of such radii that when a voltage difference V is applied between them and a particle of charge number z traverses them along the arc of a concentric circle, the energy of the particle is given by

$$E=20.00zV, \tag{3}$$

where E is in electron volts and V is in volts. The outer surface of the analyzer is held at the same potential as the target, namely ground potential, and the inner surface is maintained at a potential $-V$; hence, the energy of the particle before it enters the field of the analyzer is not the same as its energy when it traverses the analyzer. The true energy of a positively charged particle before entering the analyzer is determined by subtracting a positive correction Δ from its energy within the analyzer, whence

$$E_{\text{true}}=20zV-\Delta. \tag{4}$$

It has been thought for some time that the best value for Δ is about $0.20zV$. Recent work by Argo[6] on a similar analyzer, however, indicates that Δ more probably has the value $0.50zV$. Hence we use the relation

$$E_{\text{true}}=19.5zV \tag{5}$$

in these experiments.

The analyzer does not, of course, possess

[10] S. K. Allison, L. S. Skaggs, and N. M. Smith, Phys. Rev. **54**, 171 (1938).

perfect resolving power; that is to say, its "window curve" is not a δ-function. Instead, the analyzer window curve is nearly an isosceles triangle of half-width ΔV given theoretically by

$$\Delta V = 0.025 V. \quad (6)$$

This theoretical value is well realized in practice under good conditions.[5]

The potential $-V$ applied to the energy analyzer is produced by half-wave rectification of the output of a 100-kv transformer fed by a 540-cycle synchronous M-G set. This potential, smoothed by a filter capacitance of $0.1\mu f$, is continuously variable from 0 to 50 kv and is measured by means of the current it produces through a stack of Shallcross precision resistors. For values of V above about 20 kv, this stack consists of ten units, each of 5.0 ± 0.1 percent megohm resistance, making 50 megohms in all. For values of V below 20 kv, only four units of the stack are used. The current is measured using a Simpson d.c. ammeter, 1.5 ma full scale, with a 6-in. scale, approximately. A current of $2(10)^{-6}$ amp. through this meter produces a measurable deflection. The meter movement has been carefully calibrated, and its accuracy is therefore limited only by its sensitivity.

The potential V has a tendency to fluctuate slightly, but can be manually held within ± 100 v at 30 kv.

E. The Electron Multiplier Tube

The electron multiplier tube which detects the particles emerging from the analyzer is the same one studied and described by L. Del Rosario.[5] The external amplifying and scaling circuits are also the same that she used. The tube is mounted at the back of the analyzer in such a way as to catch on the first electrode the particles emerging from the analyzer. Each such particle then initiates the well-known cascade of secondary electrons down the series of electrodes in the multiplier tube. The output pulse from the multiplier tube is electronically amplified and is recorded by a conventional scale-of-64 circuit. To keep the background count within convenient limits, the apparatus was adjusted throughout these experiments so as to accept pulses from

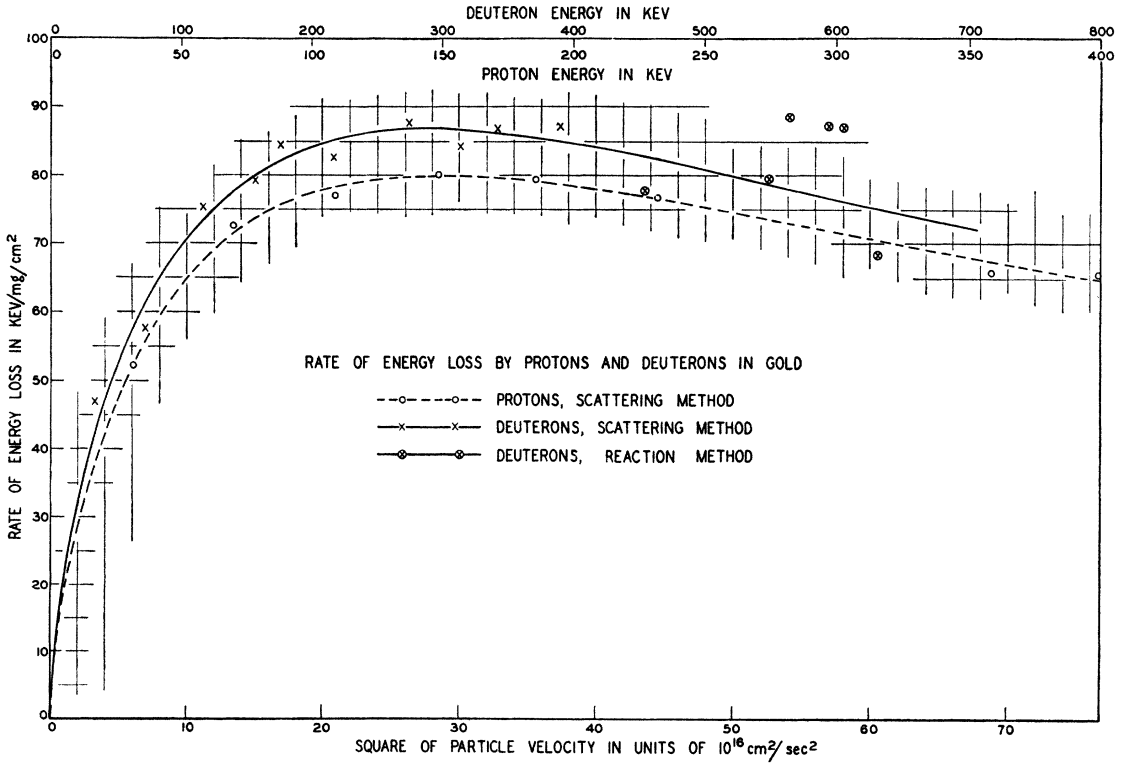

FIG. 5. Energy loss rates for protons and deuterons in Au.

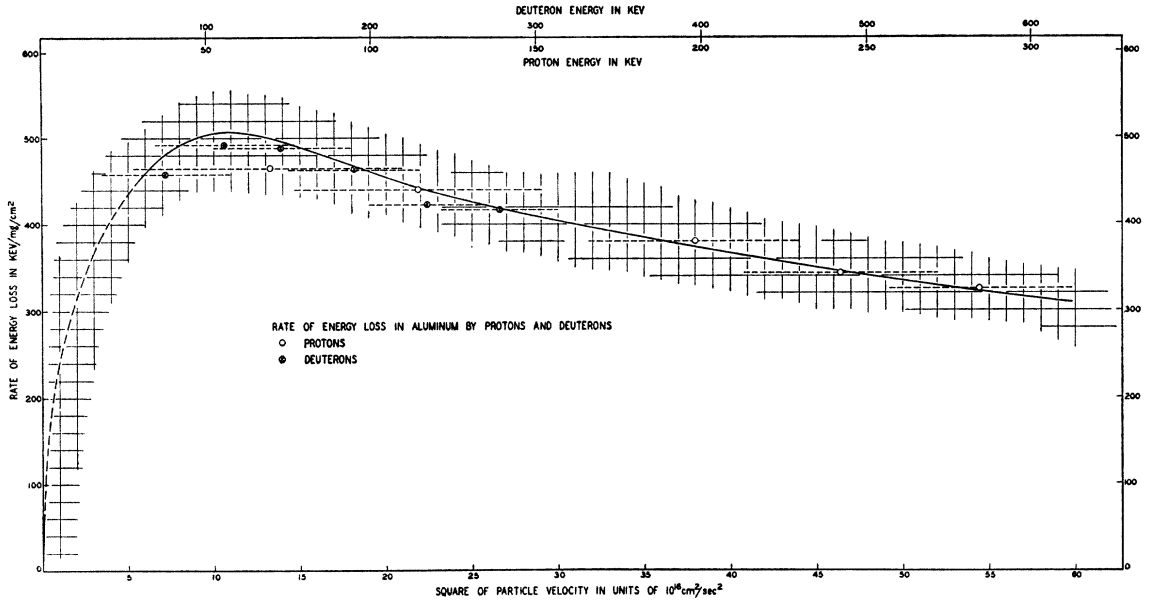

FIG. 6. Energy loss rates for protons and deuterons in Al. The experimental ordinates are the average rates of energy loss over the energy intervals indicated by the horizontal dotted lines. See text for explanation as to why the curve is not drawn through the experimental points.

the electron multiplier tube only if they exceeded approximately 20 millivolts in amplitude.

F. Method of Taking Data

In typical operation, for each setting of the analyzer potential V the scaler is permitted to count until a predetermined quantity of beam charge, as measured by the beam current integrator (Fig. 1), has been collected on the target. In this way the relative number of particles incident on the analyzer, per unit beam charge, is determined as a function of the analyzer voltage V, which therefore gives, with the aid of Eq. (5), the energy spectrum of the particles incident on the analyzer.

The carbonization of the targets, mentioned in reference 9, causes the energies of the various particles leaving the targets to decrease slowly with time. Hence the data are actually taken by first observing the energy spectrum without the foil and noting the times at which the various peaks are observed; the energy spectrum with the foil interposed is then observed and the times of observation are again noted; finally the foil is removed and the first procedure repeated. Assuming the carbon thickens at a constant rate, it is then a simple matter to calculate from these data the energies of the particles incident on the foil at the same time as their emergent energies are observed.

III. EXPERIMENTAL RESULTS, DISCUSSION, CONCLUSIONS

Figure 3 gives typical data from the reaction method. The top curve gives essentially the energy spectrum of the particles from the Be-proton reactions before the foil is interposed, the middle curve gives the energy spectrum of the particles as they emerge from the Au foil, and the bottom curve gives the spectrum after the foil has been again removed. The times of observation of the various peaks are noted in the figure. The top and bottom curves are not quite identical because of the progressive carbonization of the targets mentioned above.

It will be observed that in the top curve of Fig. 3, for example, the various peaks in the energy spectrum are identified as belonging to doubly ionized Li^6 atoms of 870-kev energy, to singly ionized H^2 atoms of 640-kev energy, and to doubly ionized He^4 atoms of 1370-kev energy. If the analyzer voltage scale in this figure were extended in both directions, additional peaks would appear belonging to the singly and triply

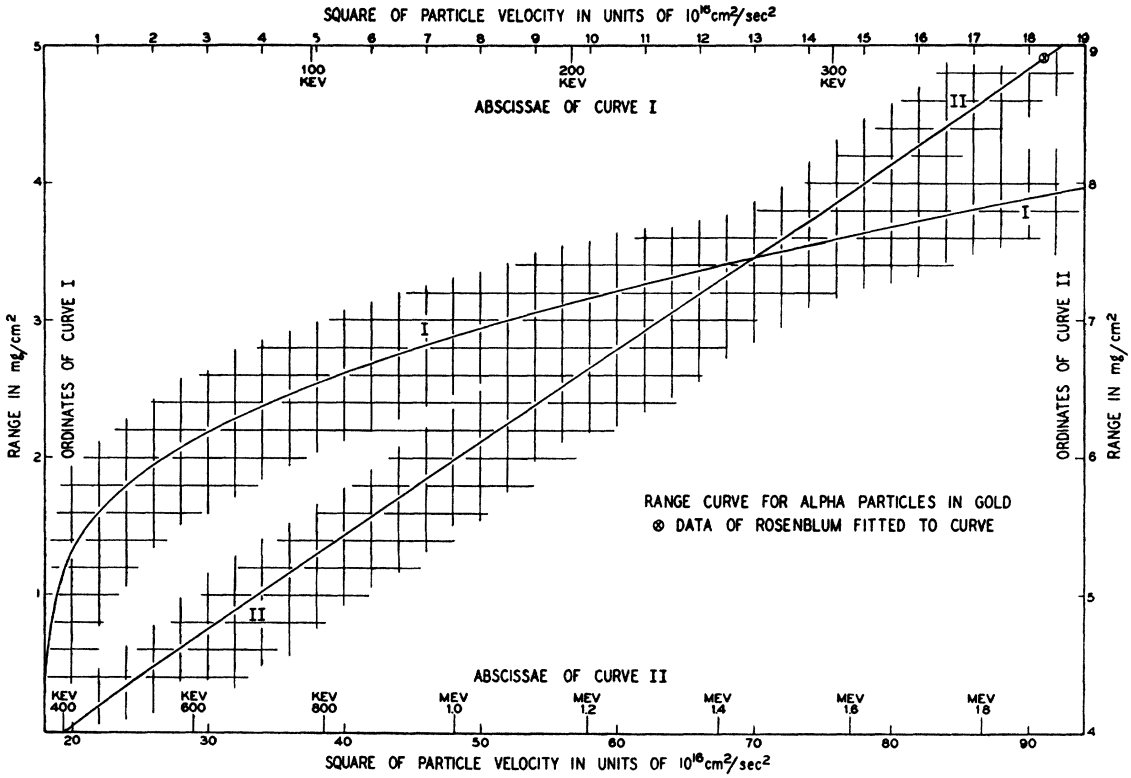

A

ionized Li^6 atoms of 870-kev energy and also to the singly ionized He^4 atoms of 1370-kev energy.

It should be noticed that the state of ionization of the various atoms before entering and after leaving the foil will have no effect whatsoever upon the rate at which they lose energy within the foil. This statement follows from the fact that inside the foil the mean free path for capture and loss of electrons is extremely short for low energy particles—hence each particle, regardless of its initial state of ionization, will capture and lose electrons hundreds of times before emerging from the foil. Upon leaving the foil, the particles will be statistically distributed among the various possible charge states in a way which depends upon their emergent energy and the surface character of the foil, but not upon their charge states when they entered the foil.

This statement is experimentally confirmed by observing the energy shifts of the various peaks when the foil is interposed. It is found, for example, that the particles in the singly ionized Li^6 peak lose exactly the same energy as the particles in the doubly ionized Li^6 peak.

Figures 4–6 give the direct results of these experiments, together with some of the results of previous investigations. In these figures $\Delta E/\Delta x$ is plotted against the square of the velocity of the particles, since current theory[1] predicts that over most of the energy range $\Delta E/\Delta x$ in a given substance will be a function only of the square of the velocity of the particle (and also of its charge number z). The "thickness" Δx of the foil is for convenience left in the form of a surface density.

The results in Fig. 4 fit in well with results derived from the work of Rosenblum[11] at higher energy.

At the very low energies obtained here, the decreased rate of energy loss by the particles immediately suggests an extrapolation to zero rate of energy loss at zero velocity; hence these figures have been so extrapolated. This procedure permits the numerical calculation of the integrated range x as a function of the particle

[11] S. Rosenblum, Ann. de physique **10**, 408 (1928).

energy, according to the formula

$$x(E)=\int_0^E (dx/dE)dE. \tag{7}$$

Integrated ranges in Au and Al are given in Figs. 7–9 for the various particles.

The stopping power of the very thin Au foil used was so small that with a high degree of accuracy the average slopes $\Delta E/\Delta x$ over the small intervals $\Delta E=E_1-E_2$ can, in Figs. 4 and 5, be identified with the true slopes dE/dx at the arithmetic mean energies $E=\frac{1}{2}(E_1+E_2)$. In the case of the available Al foil, however, the average slopes $\Delta E/\Delta x$, over the rather large energy intervals made necessary by the thickness of the foil and indicated by the horizontal dotted lines in Fig. 6, cannot always be correctly identified with the true slopes at the arithmetic mean energies; hence the curve in Fig. 6 is not drawn precisely through the experimental points. This effect is easy to take into account, and a direct check of the average slopes on Fig. 9 shows it to be correct.

In these experiments, the main uncertainty in $\Delta E/\Delta x$ stems from the fact that ΔE is the small difference of two large numbers. Hence fluctuations in the kevatron voltage and in the analyzer voltage may cause relatively large errors in ΔE. Another source of error, peculiar to the "reaction method," arises from the unavoidable straggling of the particles in the rather thick foil used to control their energies in the manner explained in Section 2 under IIB above. Hence, in this method the energy peaks are rather broad and their exact centers are difficult to locate precisely. It is thought that this effect accounts for the increased scatter of the "reaction method" points over that for the "scattering method" points, as is clearly evident in Figs. 4 and 5.

Despite these effects, however, the curves obtained are surprisingly smooth. With sufficiently great care in the regulation of the kevatron voltage and in the regulation and measurement

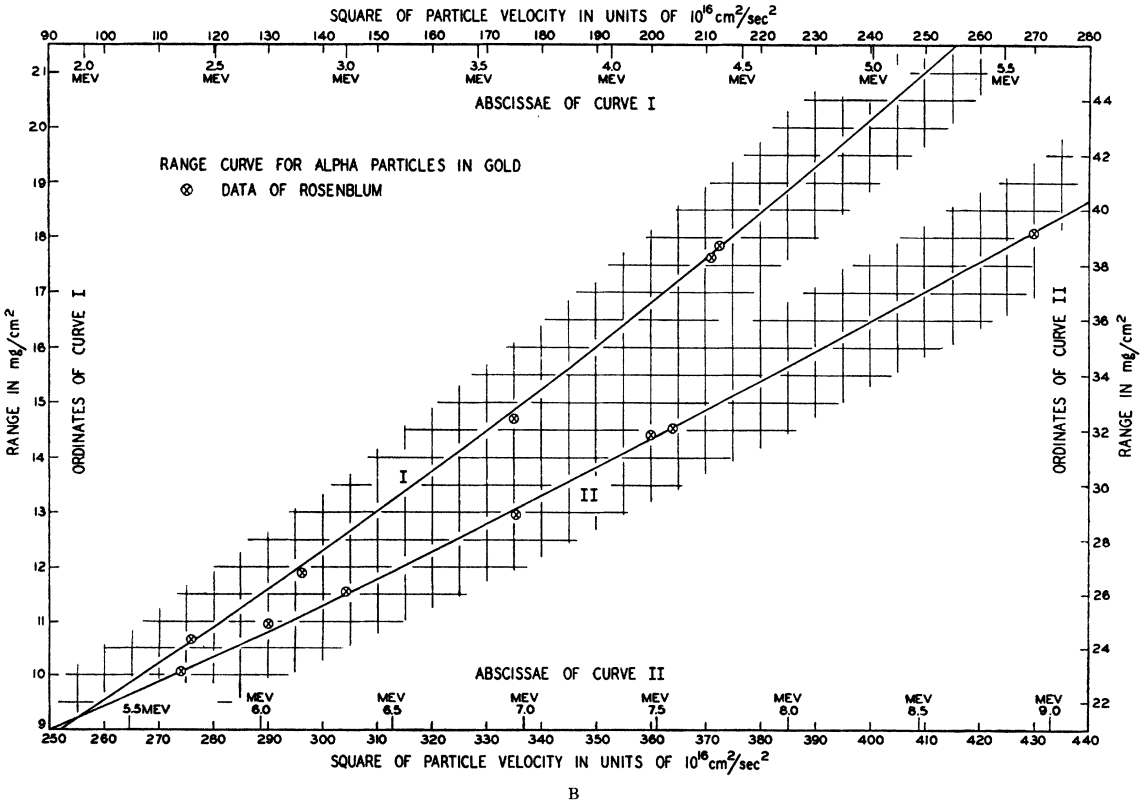

B

FIG. 7A–B. Range curve for alpha-particles in Au. From 0 to 2 Mev, the curve is obtained by numerical integration of the curve of Fig. 4; above 2 Mev the curve is obtained from the data of Rosenblum (reference 11).

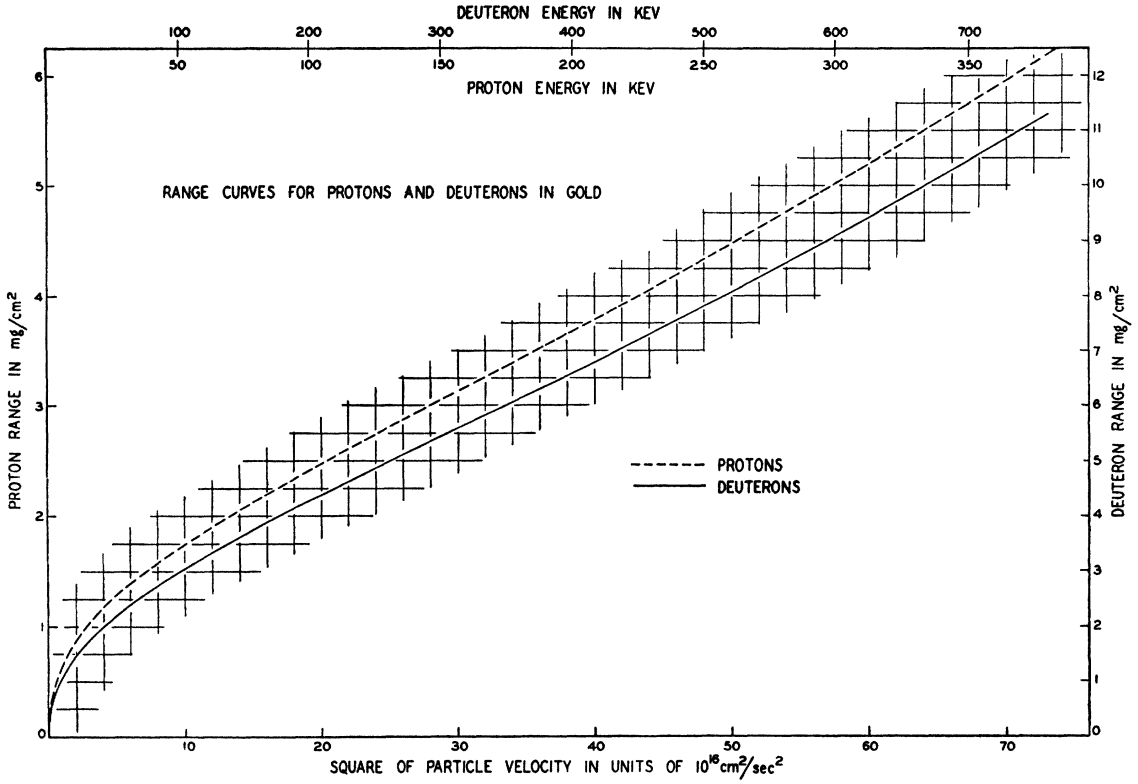

FIG. 8. Range curves for protons and deuterons in Au, obtained by numerical integration of the curves of Fig. 5.

of the analyzer voltage, it is felt that the precision of these methods can probably be improved many-fold.[12]

The most striking result of these experiments, apart from the very low energies to which they have been carried, lies in the fact that the energy loss curves for protons and deuterons in Au, Fig. 5, though very similar, are not quite identical; indeed, the maximum energy loss rate for deuterons is higher than that for protons by ~8.5 percent.

Although the similar data for Al, given in Fig. 6, are not as conclusive as the Au data because of the large energy intervals ΔE made necessary by the thickness of the available Al foil, nevertheless there seems to be evidence for the existence of the effect in Al also. In fact, the ordinate of the lowest velocity proton point in Fig. 6 is actually less by about five percent than would be predicted for a corresponding deuteron from the average slope of the integrated deuteron curve of Fig. 9. Furthermore, the slope of the proton range curve of Parkinson *et al.*,[4] given in Fig. 9, indicates a lower rate of energy loss by protons than by deuterons of the same velocity.[13]

[12] These methods can, moreover, be extended to measure the stopping power of any material which either is able to stand alone in the form of a sufficiently thin foil, or can be deposited on the very thin Au foil which is commercially available. In the latter case, a correction for the stopping power of the Au foil is easy to make since the rate of energy loss in Au is now known for protons, deuterons, and alpha particles of very low energies.

It seems likely that, by observing the relative numbers of particles in the various states of ionization as they emerge from the media, these methods can also be extended to get useful information regarding the probabilities for the various possible states of ionization of charged particles traversing solid media. This investigation is impeded at present chiefly by lack of quantitative information regarding the counting efficiency of the electron multiplier tube as a function of the energy of the incident particle, its charge, the pressure in the tube, the operating potentials for the tube, etc.

[13] In regard to Fig. 9, it should be noticed that if the rate of energy loss for protons is less than that for deuterons of the same velocity, then the proton range curve should lie above the deuteron range curve rather than below it (cf. Fig. 8). The explanation for this discrepancy may be the following: the data of Parkinson *et al.* were obtained by observing the energies of protons incident on various Al foils under such conditions that the beam currents were observed just to cease penetrating the foils. The thicknesses of the foils were then regarded as the ranges in

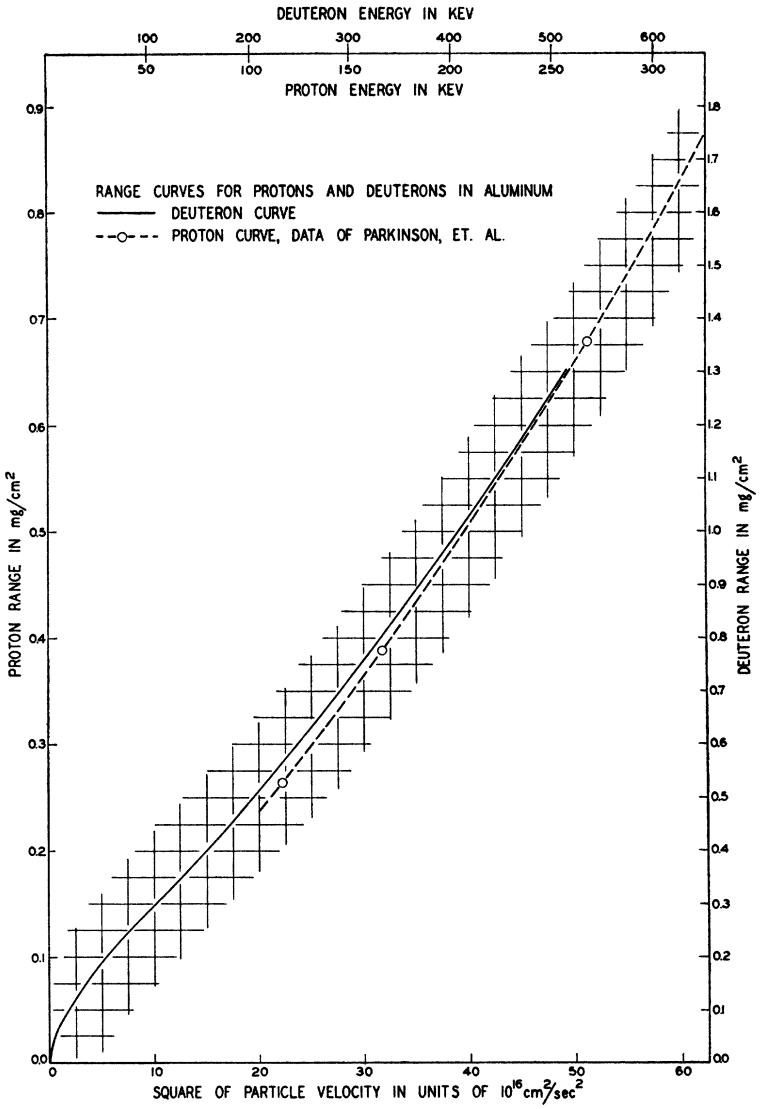

FIG. 9. Range curves for protons and deuterons in Al. The proton curve is obtained from the data of Parkinson, *et al.* (reference 4); the deuteron curve is obtained by numerical integration of the curve of Fig. 6.

The fact that the energy loss rate for deuterons is slightly higher than that for protons of the same velocity, in the region of low velocities investigated here, is in direct contradiction to the prediction by current theory that the energy loss rates for isotopic particles will be exactly the same for all equal velocities. A qualitative explanation for this difference is perhaps to be found in the mechanism of glancing, essentially "hard-sphere," elastic atomic collisions, which is entirely neglected in the usual theory. Since it is to be expected, of course, that the rather crude hard-sphere atomic model will be a fairly valid approximation only for atomic collisions in which the transfers of energy are rather small, it follows that, for incident particles of given velocity, the mechanism of hard-sphere collisions would be limited to quite glancing collisions, for otherwise the transfers of energy would be so large as to invalidate the model. As the velocity of the

Al of protons of these energies. As they point out (p. 78), however, it is likely that the proton charges are largely neutralized before the protons are stopped; and if this be the case, they will underestimate, by a small additive constant, the range in Al of protons of every energy they used. Hence it is possible that the proton curve of Fig. 9 should be shifted upward by adding to every range ordinate a small constant.

incident atoms decreases, on the other hand, the hard-sphere model would become valid for more direct collisions and hence for an increasing fraction of the total number of collisions; therefore this mechanism would become relatively more important in the energy losses of low velocity particles than in the losses of high velocity particles, where it may justifiably be neglected.

On the basis of the hard-sphere model, elementary considerations show that a deuteron loses, on the average, about four times as much energy as does a proton of the same velocity, in a (glancing) collision with a heavy atom at rest. Clearly, then, this mechanism would contribute to an increased rate of energy loss for deuterons compared with that for protons, as observed.

IV. ACKNOWLEDGMENTS

I wish to thank Dr. S. K. Allison, in whose laboratory this work was done, for his constant interest and valuable advice in the course of the work. In addition, I wish to express my thanks for the very important and active help of Mr. C. N. Yang during the early phases of these investigations. Finally, thanks are due Messrs. D. S. Bushnell and G. W. Farwell for their assistance with the tedious but necessary job of taking the many data.

PHYSICAL REVIEW VOLUME 74, NUMBER 12 DECEMBER 15, 1948

Search for Photons from Meson-Capture*

O. PICCIONI**
Laboratory for Nuclear Science and Engineering, Massachusetts Institute of Technology, Cambridge, Massachusetts
(Received August 27, 1948)

High energy photons (about 50 Mev) associated with mesons stopped in iron have been searched for. The experimental evidence shows that no such photons arise from the capture of negative mesons or from the free decay of positive ones.

EXPERIMENTS with delayed coincidences[1] have shown that no decay electrons are detected from negative μ-mesons stopped in materials with high Z. This was predicted by Tomanaga and Araki, in line with Yukawa's theory.[2] Their conclusion was that negative mesons at the end of their range should be attracted by the Coulomb field of the nuclei and then "captured" by the nuclei even for low values of Z and density of the absorber. The presence of decay electrons for both positive and negative mesons in light nuclei already indicates a strong departure from the predictions of Tomanaga and Araki and hence from Yukawa's theory, as far as μ mesons are concerned. However, the event following the capture of negative μ-mesons in a high Z absorber was somehow expected to undergo the process which was predicted on the basis of Yukawa's theory. This process should most likely lead to a nuclear disruption in which the outgoing particles would carry almost all of the 100 Mev rest energy of the mesons. From the absence of such stars in cloud chamber pictures, it was felt[3] that the idea sketched above does not correspond to the actual phenomenon.***,[4] Hence the present experiment

* Preliminary results of this work appeared in Phys. Rev. **73**, 411 (1948); a complete report was given in the Washington meeting of the American Physical Society, April 29, 1948.

** Now at Brookhaven National Laboratory, Upton, Long Island, New York.

[1] Conversi, Pancini, and Piccioni, Phys. Rev. **68**, 232 (1945); G. E. Valley, Phys. Rev. **72**, 772 (1947).

[2] Tomanaga and Araki, Phys. Rev. **58**, 90 (1940).

[3] O. Piccioni, Phys. Rev. **73**, 411 (1948).

*** After this experiment was performed, Lattes and Gardner (see reference 4) reported that μ mesons had been detected with photographic plates exposed in the 184-inch cyclotron of Berkeley. Only a part (<50 percent) of the observed μ mesons produce a star at the end of their range, and these stars have mostly one prong. From the comparison with the Σ-stars, one has the impression that the μ-stars do not represent an energy of 100 Mev. Other information on this subject is available from the preliminary results of R. Sard and coworkers, who find neutrons associated with the stopping of mesons in lead. Unfortunately quantitative information is not available as yet.

[4] Lattes and Gardner, Am. Phys. Soc. **23**, No. 3, p. 42 (1948).